Nanostructured TiO_2-based Anode Materials for High-performance Rechargeable Lithium-ion Batteries

Yanyan Zhang, Yuxin Tang, Wenlong Li, and Xiaodong Chen*

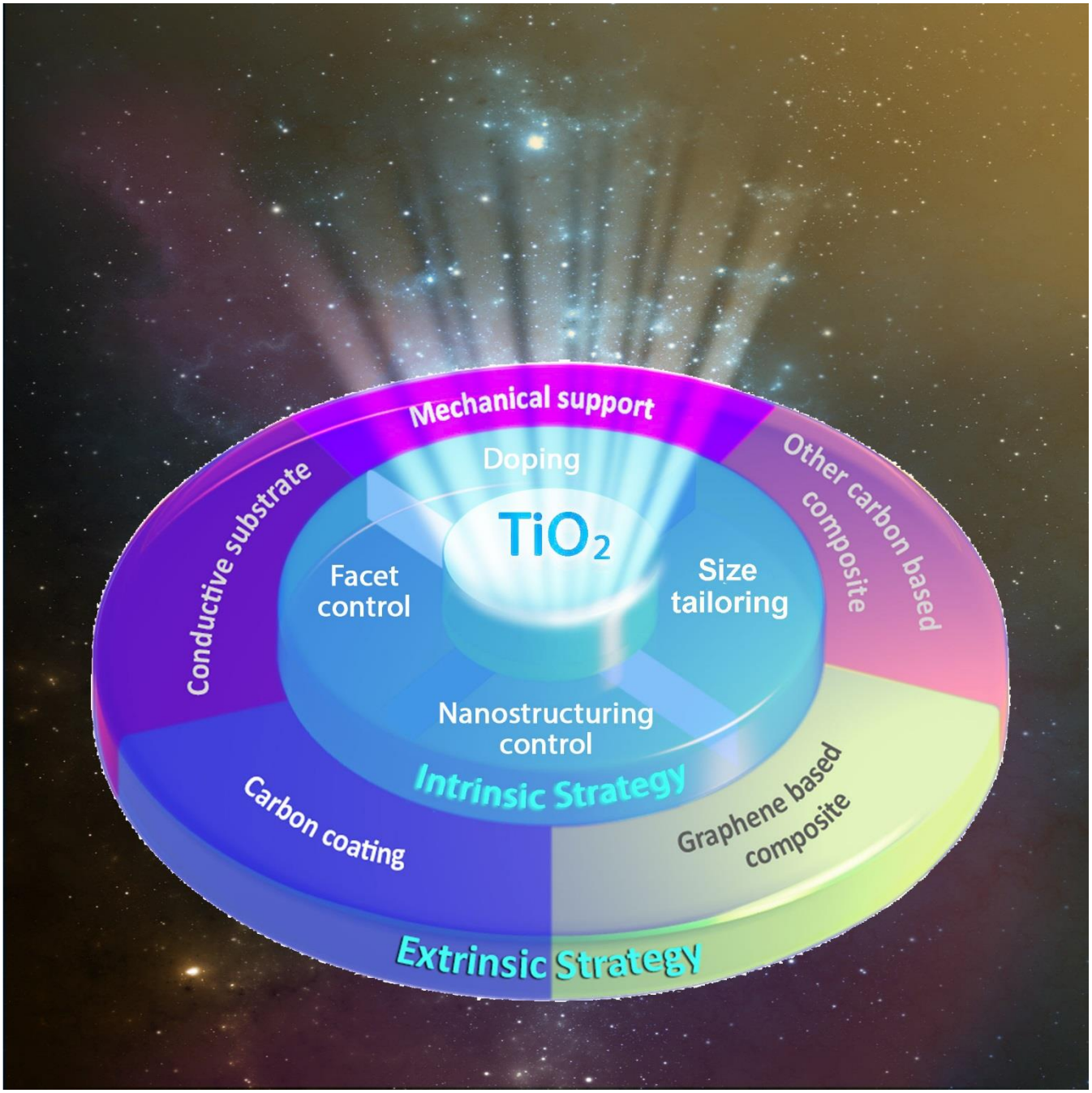

Abstract: Lithium ion batteries (LIBs), as the most widely applied power source for the portable electronics and electric vehicles industry, are expected to advance with a high standard in terms of high safety, long lifespan, high energy density and high power density. However, the commercial graphite anode is still suffering from the potential safety issues. To address this challenge, the TiO_2–based materials are widely explored as anode electrode and the promising progress is achieved in the past few decades. In this review, we present the state-of-the-art materials design strategies on TiO_2 materials to achieve high performance LIBs. Firstly, a brief discussion on basic requirements for LIBs is introduced as a prerequisite. Secondly, for the purpose of improving the electrode performance of TiO_2 materials, the corresponding material engineering approaches are illustrated, which include intrinsic methods and extrinsic approaches. Lastly, the challenge and future perspective for the nanostructured TiO_2 toward high-performance of LIBs are outlined. This review is expected to give a comprehensive understanding and guidance on TiO_2-based materials in the application of energy storage devices.

1. Introduction

Lithium-ion batteries (LIBs) have been widely applied in the portable electronics and automotive industry owing to their high energy density (> 180 W h kg^{-1}),[1] and they are regarded as an effective strategy to reduce CO_2 emission and environmental pollution. Conventional LIB cells are assembled from graphite anode and $LiCoO_2$ cathode with a porous membrane separator immersed in electrolytes, within which lithium ions shuttle between electrodes while electrons circulate among external loads during charging/discharging cycles. To cater for various applications, high power/energy density and long cycle life are of vital importance for LIBs.[2] However, graphite anode is still suffering from the potential safety issues (thermal runaway), with the formation of lithium dendrites and solid-electrolyte interphase (SEI) layer, due to its low lithiation potential (0.2 V vs. Li/Li^+), especially when the LIBs are operated at high current rates.[3] Therefore, the seeking on a suitable electrode material addressing the above challenges is desired.

The desired battery performances include high safety, long lifetime, high energy density and high power density (Figure 1). These factors are associated with each component of the battery (such as electrode materials, separator and electrolyte) as well as the operating conditions.[4] To meet the above four key requirements, the nanostructured TiO_2-based anode material is promising compared with the commercial graphite with safe lithiation potential, comparable capacity, long cyclability, and superior rate capability. Therefore, this review paper focuses on the TiO_2 anode materials for LIBs, and the considerations from the material aspect towards high performance LIBs are highlighted.

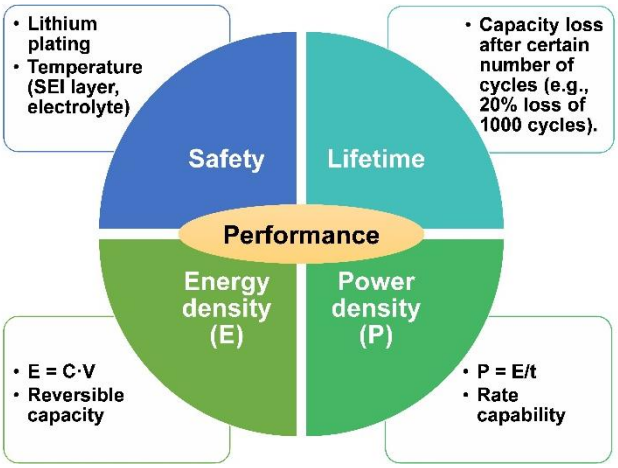

Figure 1. Schematic representation of the key merits for battery performance, including high safety, long lifetime, high energy density and high power density.

Possessing elevated operating potential (above 0.8 V vs. Li/Li^+),[3, 5] TiO_2 materials are capable of avoiding lithium plating and prohibiting decomposition of the electrolyte, rendering them as the promising safe anode material candidates for LIBs. Moreover, TiO_2 materials show negligible structural stain and small volume change (<4%) upon lithiation/delithiation processes,[3, 5b] making them highly stable with long cycle life. To date, three TiO_2 polymorphs including rutile, anatase, and TiO_2-B (bronze) have been reported as the anode materials (Table 1).[3a] Rutile (tetragonal, $P4_2/mnm$) is the most thermodynamically stable phase, however, studies have shown that in bulk form, only small fraction of lithiation sites in rutile can be accessed because half of the interstitial octahedral sites are occupied to form coordinated TiO_6 octahedral, resulting to low theoretical capacity of 33.5 mAh/g ($Li_{0.1}TiO_2$). Furthermore, the channel along the *c* axis in rutile TiO_2 is too narrow for lithium ions to transport, and the diffusion coefficient in the *ab* plane (10^{-15} cm^2/s) is nine orders smaller than that in *c* direction.[6] All these drawbacks lead to poor performance of bulk rutile TiO_2 materials. Compared to rutile, anatase polymorph (tetragonal, $I4_1/amd$) offers much higher specific capacity of 167 mAh/g even in bulk form, corresponding to $Li_{0.5}TiO_2$. Nanostructuring the material could further enhance the surface storage behavior and improve the overall capacity to 285 mAh/g.[7] During the charge/discharge processes, Li^+ ions insert/extract into/from anatase through solid-state diffusion, potentially deteriorating its high rate performance. Among these commonly used polymorphs, TiO_2-B (monoclinic, C2/*m*) has the highest theoretical capacity up to 335 mAh/g. Compared to rutile and anatase TiO_2, TiO_2-B contains open channel structure, which is beneficial to pseudocapacitive Li^+ ions storage. There are more sites inside TiO_2-B that can accommodate Li^+ ions, denoted as A1 (distributed at the vicinity of TiO_2 layers parallel to the *ab*

Dr. Y. Zhang, Dr. Y. Tang, Mr. W. Li, Prof. X. Chen
School of Materials Science and Engineering
Nanyang Technological University
50 Nanyang Avenue, Singapore 639798, Singapore
E-mail: chenxd@ntu.edu.sg

plane), A2 (distributed at the vicinity of O layers parallel to the *ab* plane), and C (arranged in infinite channels along *b* axis).[8] Such open channel enables improved diffusion kinetics of Li^+ ions and favoring Li-ion insertion even in bulk form. The main drawbacks of all TiO_2 polymorphs stem from their poor electronic conductivity and low Li-ion mobility due to the large bandgap and high ion diffusion energy barrier, respectively (Table 1).

Table 1. Diffusivity and electronic conductivity of graphite and TiO_2 polymorphs.

Anode materials	Diffusivity ($cm^2\ s^{-1}$)	Electronic conductivity ($S\ cm^{-1}$)
Graphite	10^{-10} - 10^{-9} (room temperature) [9]	10^3 [9]
Rutile TiO_2	10^{-6} (*c*-direction)[10]	
	10^{-10} (a-direction)[10]	
Anatase TiO_2	10^{-16} [10, 12]	10^{-12} [11]
	10^{-13} (single crystal)[10]	
	10^{-10} - 10^{-17} (films)[10]	
	10^{-12} [13]	
TiO_2-B	10^{-7} [14]	

To address the above challenges, we review on the state-of-the-art strategies regarding materials design on TiO_2-based electrode materials towards high performance LIBs. Firstly, the general approaches on TiO_2-based anode materials for high performance LIBs are given. Secondly, guided by the requirements aforementioned, the corresponding approaches adopted to intrinsically and extrinsically engineer TiO_2 based materials for LIBs are illustrated. Lastly, future challenge as well as perspectives regarding TiO_2-based electrode materials are outlined.

2. Design strategies on Nanostructured TiO_2–based electrode materials

Titania-based materials, with the structures built on different edge-/corner-sharing TiO_6 octahedral configurations, show good cycling stability owing to zero strain and low volume expansion (< 4%) upon lithiation/delithiation.[3b, 5b] However, their poor electronic (10^{-12} S cm^{-1})[11] and low Li-ion diffusion coefficient (10^{-6}~10^{-17} $cm^2\ s^{-1}$)[10, 12-14] limit their performance. Therefore, rational design to enhance migration kinetics of the electrons and Li-ions within the TiO_2 electrode materials are with critical importance for high-performance LIBs. This can be realized by either intrinsically tuning their properties or extrinsically hybridizing with other compounds. The detailed approaches are summarized in Figure 2.

Figure 2. Intrinsic and extrinsic strategies on materials design towards high performance LIBs.

2.1 Intrinsic engineering on TiO_2 materials

The physicochemical properties of materials is influenced by their size, phase, morphology, structure, and so on.[15] For instance, as particle size goes down, more surface areas are exposed, corresponding to more available sites for electrochemical reaction to take place. Particularly, reducing particle size to nanoscale gives rise to tremendous active surface thus greatly outperforms those in bulk form. Hence, though TiO_2 materials are suffering from poor ionic/electronic conductivity which limits the lithium storage rate, the transport of electrons and Li^+ ions can be promoted by rational engineering of their physicochemical features (Figure 3), such as size tailoring, structure/morphology optimization, facet controlling, and electronic structure manipulation.

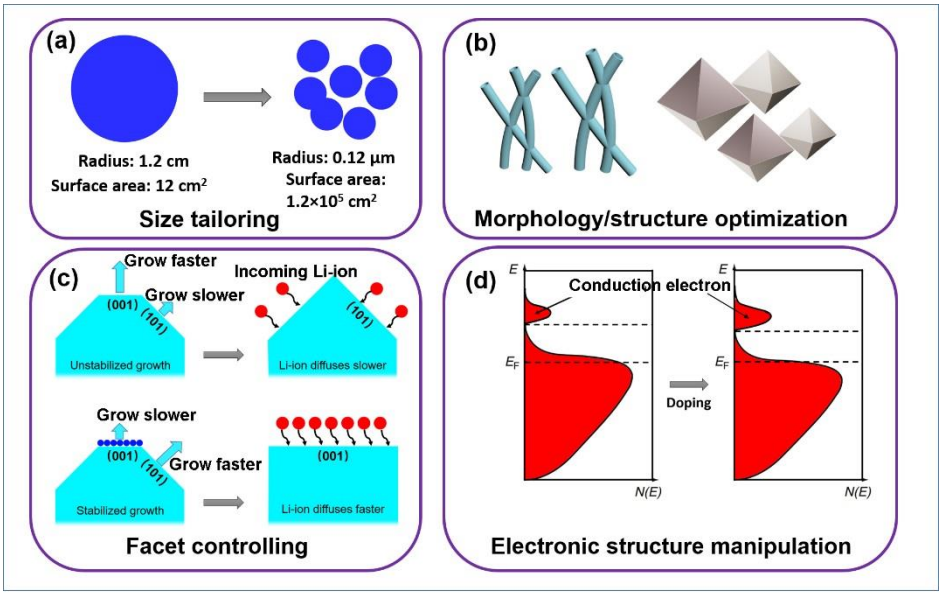

Figure 3. Intrinsic strategies towards high performance of TiO_2 materials, including the size tailoring, structure/morphology optimization, and facet controlling, etc.

2.1.1 Size tailoring

From atomic perspective, the rate performance is determined by the diffusive movement of Li^+ ions in energy-favored pathway of the material. As we discussed above, the diffusion time (τ) of Li-ion in electrode materials is proportional to the square of the diffusion length (λ) according to the equation $\tau = \lambda^2/D_{Li}$.[1d] Hence, reducing the material size to nanoscale (Figure 3a and 4a) is a seemingly straightforward way to produce immediate effect on the rate performance. On one hand, nanomaterials with reduced size have shorter diffusion length, thus the time to saturate all the available sites is reduced. On the other hand, nanomaterials are also benefited from high surface area compared to bulk materials, and they are most likely to be active and accessible for electrolyte impregnating, allowing more Li^+ ions to be transported through the electrolyte/electrode interface. For example, TiO_2-B nanoparticles with the particle size of 2.5 × 4.3 nm and surface area of 251 $m^2\ g^{-1}$ exhibited superior volumetric capacity at all rates compared to the 6 nm anatase material and the previously reported best high rate (> 1 A g^{-1}) volumetric capacity (Figure 4b-c).[16]

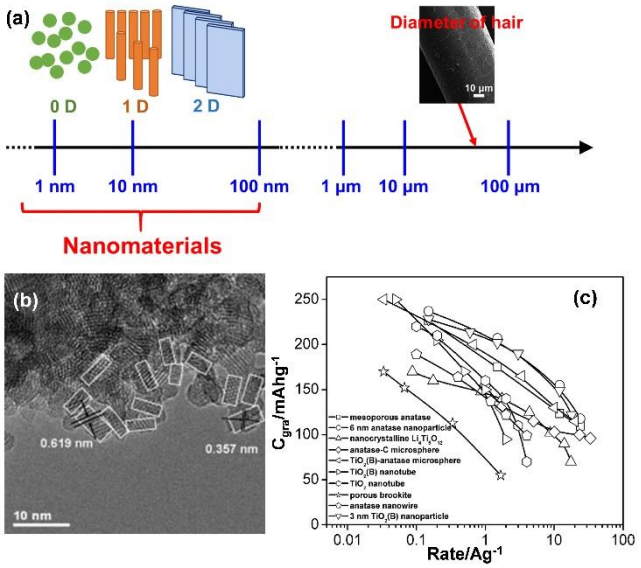

Figure 4. Size tailoring of TiO_2 electrode materials: (a) Nanostructured materials serving as the electrode materials. (b) HRTEM image of TiO_2(B) nanoparticles. White boxes delineate primary nanoparticles within the agglomerates; and (c) Gravimetric capacity of TiO_2(B) nanoparticles compared with other titanate materials as a function of rate.[16]

2.1.2 Morphology/structure optimization

Nanomaterial morphology and structure control makes impressive progress for the TiO_2 anode materials (Figure 3b). Up to date, zero-dimensional (0D) nanospheres, one-dimensional (1D) nanostructures, two-dimensional (2D)

nanoarchitectures and three-dimensional (3D) hierarchical nanostructures sprung up aiming to enhance the transport rate of electrons and Li^+ ions. These nanostructures possess the advantages of providing high contact surface area with the electrolyte as well as short diffusion pathways for electrons and Li^+ ions. Recently, we reported that the elongated TiO_2 nanotubes with the length of 30 μm (Figure 5a-b) possessed high capacity of 114 mAh g^{-1} at 25 C over 10000 cycles (Figure 5c).[17] Furthermore, we revealed that the nanotubular aspect ratio played a critically important role in the electrochemical performance (Figure 5d).[18] The battery performance was significantly promoted along with the increase of the aspect ratio, which can be ascribed to the optimization of the electronic and ionic transport properties within the electrode materials. Remarkably, other structures, such as TiO_2 hollow microspheres (Figure 5e-f) and so on,[3b, 19] are also of importance for electrode materials of LIBs, manifested superior lithium storage properties in terms of high specific capacity, long cycling stability, and excellent rate capability. For example, uniform TiO_2 nanospheres from hollow, core-shell and mesoporous structures have been developed recently,[19b] and the hollow and mesoporous TiO_2 nanospheres delivered discharge capacities of 103.0 and 110.2 mAh g^{-1} respectively, even after 3000 cycles at a current rate of 20 C.

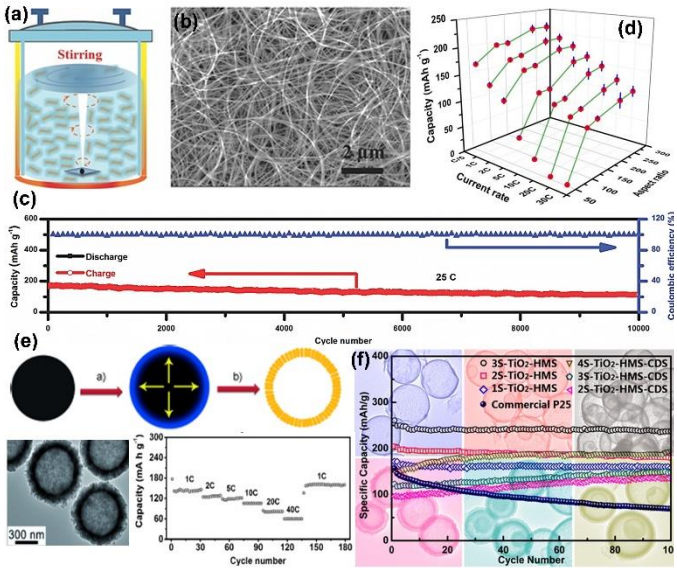

Figure 5. Morphology/structure optimization of the TiO_2 materials: (a) Scheme of the stirring hydrothermal method to fabricate elongated TiO_2 nanotubes as shown in (b), and (c) the corresponding high-rate cycling performance at 25 C.[17] (d) The correlation between the aspect ratio and the capacity of different TiO_2 nanotubes at various discharge rates.[18] (e) Illustration of the formation of TiO_2 hollow spheres using carbon spheres as templates and the TEM image of the as-prepared TiO_2 hollow spheres.[19a] (f) TEM images of multishelled TiO_2 hollow microspheres and their corresponding cycling performance.[3b]

Despite the smart design of materials with multifarious control to improve the TiO_2 battery performance, judicious design of the configuration to facilitate/enlarge the energy storage in synergy is impressive. Maier et al[20] proposed a so-called "Job-sharing" mechanism that an additional synergistic storage is favored, benefited from enhanced charge separation if the electrode material has the configuration of one Li^+-accepting phase and an e^--accepting phase. A typical demonstration is the microsphere constructed by ultrathin anatase TiO_2 (e^--accepting phase) nanosheets embedded with TiO_2-B (Li^+-accepting phase) nanodomains.[21] Additional lithium storage venues are generated based on the favorable charge separation at the boundary between the two phases. Conjugated with the fact that the reaction kinetics of an interfacial storage process can be much faster than those of a bulk lithium insertion reaction, this sample exhibited capacities of 180 and 110 mAh g^{-1} after 1000 cycles at current densities of 3.4 and 8.5 A g^{-1} respectively.

2.1.3 Facet controlling

Synthesis of nanocrystals with high energy facets is challenging in many field of science and technology (Figure 3c). It is shown that the higher reactivity facets of catalysts makes them desirable for enhancing chemical reactions.[22] For anatase TiO_2, its (001) facets (0.90 J/m^2) are more energetical than (101) facets (0.44 J/m^2).[22b] As a result, the (001) facets are more likely to form at the early stage of crystal growth and then quickly eliminate. Thus, many efforts have been explored on the synthesis of anatase TiO_2 with high percentage of exposed (001) facets. Recently an approach to construct the hierarchical structure by anatase nanosheets with high specific surface area (170 m^2 g^{-1}) and nearly 100% (001) facets exposure was reported.[22b] The first discharge capacity of 300 mAh g^{-1} was obtained at 0.5 C and a reversible capacity of 150 mAh g^{-1} was achieved at current rate of 10 C. Furthermore, anatase TiO_2 having different percentages of (001) and (101) surface (Figure 6a-b) demonstrated different behaviors for Li^+ ions insertion, and the (001) facet anatase possesses high-rate performance at 10 C (Figure 6c).[23]

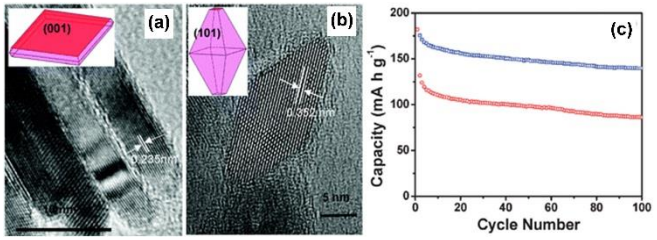

Figure 6. Facet controlling of the TiO_2 materials: (a) and (b) TEM images of the anatase TiO_2 with dominant (001) and (101) facets respectively, and (c) Cycling performance at different rates of 10 C by using anatase TiO_2 with dominant (001) facets (blue) and (101) facets (red).[23]

2.1.4 Electronic structure manipulation

The electronic conductivity of TiO_2 electrode material depends on the density of free electrons in conduction band and holes in valence band (Figure 3d). Unfortunately, the wide

bandgap of TiO_2 material (3.2 eV) limits the availability of free electrons in conduction band, giving rise to an intolerant electronic conductivity (10^{-12} S cm^{-1}). In response to this intrinsic issue, doping method is an effective strategy. By introducing foreign species (metal or nonmetal ions) or vacancies to the host material, the bandgap of host material is tuned. Indeed, a subtle decrease of the band gap energy can unleash a great amount of conductive electrons due to an exponential relationship between charge carrier concentration and band gap energy. As a result, the rate performance of TiO_2 materials is improved. For example, black anatase TiO_2,[24] fabricated by treating the TiO_2 precursor at 600 °C in the Ar atmosphere (Figure 7a-c), showed very high electrical conductivity of 8×10^{-2} S cm^{-1}, which results from the presence of Ti^{3+} in the Ar atmosphere. Consequently, the inherent bandgap of the TiO_2 is narrowed from 3.2 to 1.8 eV. The enhanced electrical conductivity ensures the rate performance of black anatase, which shows high discharge capacity of 127 mAh g^{-1} at 100 C (20 A g^{-1}) and good capacity retention of 86% after 100 cycles (Figure 7d). Doped anatase TiO_2 can also be obtained by post-treating through low-temperature (150 °C) vacuum process (Figure 7e).[25] The extension of absorption from ultraviolet region to near infrared region gives a strong evidence to prove the reducing in band gap. The electrode performance show more than 30% enhancement than pristine TiO_2 in capacity under different rates (Figure 7f).

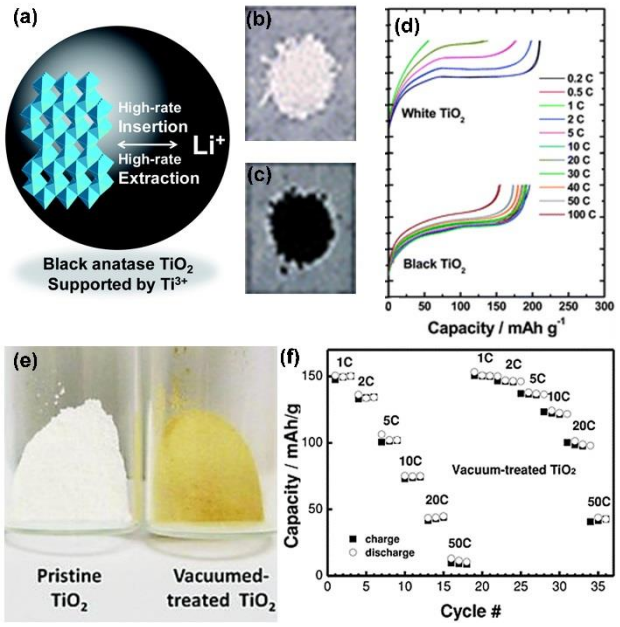

Figure 7. Dopant manipulation method: (a) Schematic drawing of the mixed valence in anatase TiO_2; digital images of the white (b) and black (c) TiO_2; and (d) comparison of the rate capability for the white anatase TiO_2 heated at 400 °C for 5 h in air and the black anatase TiO_2 during discharge.[24] (e) Digital images of the pristine and vacuum-treated TiO_2 nanocrystals; and (f) the rate performance of the pristine and vacuum-treated TiO_2 nanocrystals.[25]

2.2 Extrinsic strategies on TiO_2 materials towards high performance LIBs

Beyond the intrinsic strategy for the enhancement of Li^+ ion diffusion and electron transport, there exists extrinsic approaches to facilitate the carrier transport. To this end, surface engineering (Figure 8), including carbon coating, conductive substrate design, and hybridization with conductive agent, has been considered as the promising approaches for improving the battery performance in term of rate performance, cycling capability, and capacity.

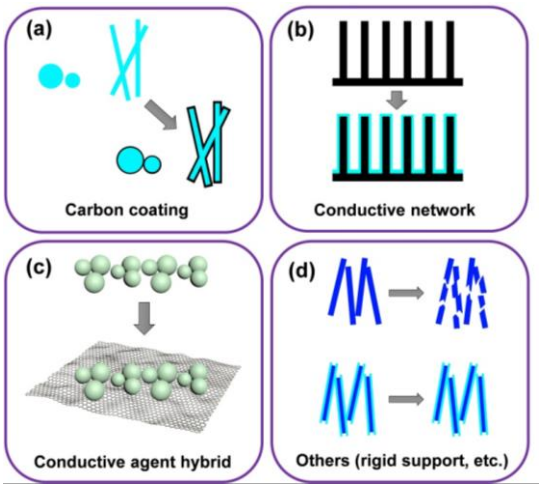

Figure 8. Extrinsic strategies towards high performance of TiO_2 materials, including the carbon coating, hybridization with metal/nonmetal compounds, etc.

2.2.1 Carbon coating approach

Carbon coating, serving as the electronic conductive layer, is considered as the typical route to enhance the surface conductivity of the active materials[26] (Figure 8a). In this case, electrons are able to access all the spots on the active material's surface while Li^+ ions can pass the coated carbon layer to reach the material surface as well. This enhances the battery performance in terms of both capacity and rate capability. Manthiram *et al.*[5b] reported mesoporous nanowire arrays composed of a carbon layer coated on TiO_2 encapsulating Sn nanowires (TiO_2-Sn/C) as high-performance 3D additive-free, self-supported anodes for LIBs (Figure 9a). The electrodes with carbon coating (TiO_2-Sn/C) show a lower ohmic resistance (2.9 Ω) and a lower charge-transfer resistance (94.3 Ω) compared to those of TiO_2-SnO_2 samples (4.1 and 151.2 Ω respectively, Figure 9a). This unique TiO_2-Sn/C core-shell composite arrays display superior rate capability that the discharge capacity reaches 90 mAh g^{-1} at 30 C and excellent long-term stability that the capacity retention rate of 84.8% with a discharge capacity of over 160 mAh g^{-1} even after 100 cycles at 10 C (Figure 9c). Likewise, Chen *et al.*[26b] demonstrated TiO_2-C/MnO_2 core-double-shell nanowire arrays as anode for LIBs (Figure 9d-e). The additional carbon coating interlayer improves the electrical conductivity, leading to the enhanced electrochemical

performance with a higher discharge/charge capacity, superior rate capability, and longer cycling lifetime.

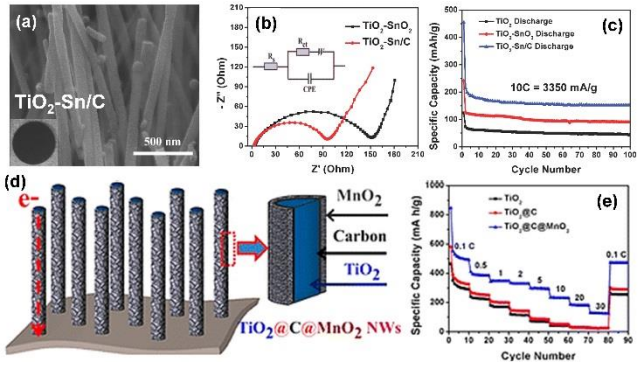

Figure 9. Carbon coating of TiO_2 materials to enhance the electronic and ionic conductivities: SEM images and digital photos of the as-prepared (a) TiO_2-Sn/C arrays; (b) Nyquist plots of TiO_2-SnO_2 and TiO_2-Sn/C electrodes in the fully charge states; (c) high-rate cyclic performance of the electrodes at 10 C.[5b] (d) Schematic illustration for the fabrication of TiO_2-C/MnO_2 core-double shell nanowire arrays and their corresponding rate performance as shown in (e).[26b]

Direct growth of TiO_2 on conductive network is regarded as an effective strategy for high-performance LIBs.[27] A unique conductive network (Figure 8b) would provide active material with faster electron transport channel, larger contact area with electrolyte, a shorter Li^+ ion diffusion length and a better accommodation space for volume change buffering. The conductive substrates with varied dimensions, allow the electron and Li^+ ion to transport through the corresponding one, two and three directions, respectively. The enhanced Li^+ ion and electron transport kinetics via the conductive network would result in outstanding electrochemical performance of the LIBs. For example, core/shell indium tin oxide (ITO)/TiO_2 nanostructured electrodes, with the growth of TiO_2 nanoparticles on the highly conductive ITO nanowire arrays were synthesized (Figure 10a).[27b] This configuration, enabling direct and short diffusion pathways for Li^+ ions and electrons, results in large reversible capacity (larger than 200 mAh g^{-1}), superior rate capabilities, and extremely low average capacity fading of ~0.01% per cycle over 1000 cycles at 60 C (Figure 10b). Using the similar concept, atomic layer deposition of TiO_2 on the interconnected conductive 3D Ni nanowire network was demonstrated for high areal capacity lithium ion microbatteries (Figure 10c).[28] Excellent capacity retention of 100% after 600 cycles was achieved with a stable Ni/TiO_2 nanowire network structure.

2.2.2 Conductive network design

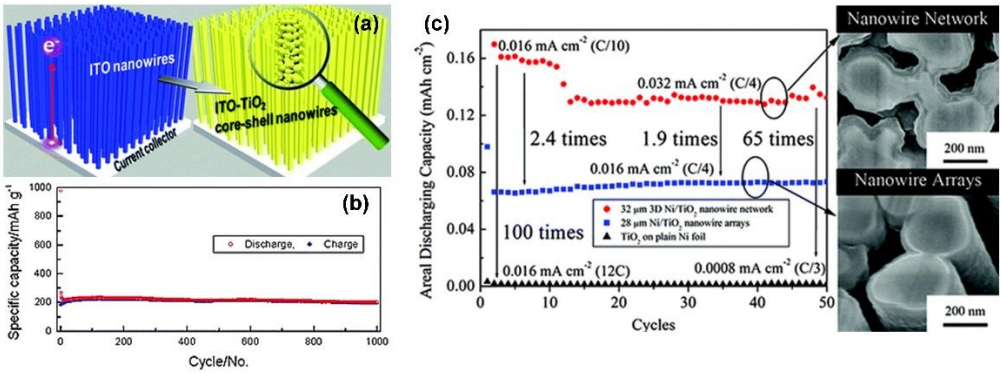

Figure 10. Direct growth of TiO_2 on conductive substrates: (a) Illustration of synthesis of ITO-TiO_2 core-shell nanowires; and (b) Variation of the discharge-charge specific capacity *versus* cycle number at 60 C for the ITO-TiO_2 core-shell nanowires electrode.[27b] (c) Areal discharging capacity of 3D Ni/TiO_2 nanowire network, straight Ni/TiO_2 nanowire arrays, and TiO_2 coated plain Ni foil.[28]

2.2.3 Conductive agent hybrid strategy

Recently, graphene, the single layer of graphite, possessing superior physicochemical properties including high electrical conductivity, large surface area, good structural flexibility, and modifiable surface functional groups, has been promising as the multifunctional substrate to promote the electrochemical performance of TiO_2. For example, sandwich-like graphene-based mesoporous TiO_2 (G-TiO_2) nanosheets[29] display an excellent rate capability and cycle performance owing to the increased electrical conductivity of the graphene component as well as the enhanced diffusion of Li^+ ions in its mesoporous structure (Figure 11a). Besides that, TiO_2 nanospheres/graphene sheets[30] (Figure 11b) shows striking high rate performance in LIBs with the specific capacity of 97 mAh g^{-1} at 50 C, which is 6 times higher than that of the reference TiO_2 (Figure 11c). Furthermore, flower-like TiO_2/graphene[31] (Figure 11d-e) and TiO_2 quantum dots / graphene nanosheets (TiO_2-QDs/GNs)[32] (Figure 11f) were achieved for high rate LIBs. Recently, the interaction between the TiO_2 and graphene was revealed as the Ti^{3+}-C chemical bonding in TiO_2-B/RGO hybrid system,[33] which provides efficient interfacial charge transfer between RGO monolayers and TiO_2-B nanosheets. Taking the advantage of strong

coupling effects between inorganic/graphene to allow precise tuning of the hybrid materials, Zhao's group[34] reported mesoporous TiO_2/graphene/mesoporous TiO_2 sandwich-like nanosheets to further enhance lithium storage. Moreover, interesting study combining the advantages of facet exposure of the TiO_2 into the graphene-based system[35] also showed outstanding high rate performance of LIBs.

Beyond the graphene-based materials, by incorporating TiO_2 with carbon-based materials (such as carbon nanotubes and carbon fabric), TiO_2/carbon hybrid composites are also explored. For instance, multiwall carbon nanotubes (MWNTs) were incorporated with the sub-8 nm TiO_2 nanoparticles,[36] and the electrodes demonstrate high capacity (> 150 mAh g^{-1} at 0.1 A g^{-1}), good rate capability (> 100 mAh g^{-1} up to 1 A g^{-1}) and negligible capacity loss up to 200 cycles for electrodes with thickness up to 1480 nm. Besides carbon nanotubes, other kinds of carbon species as the conductive substrates are also used.

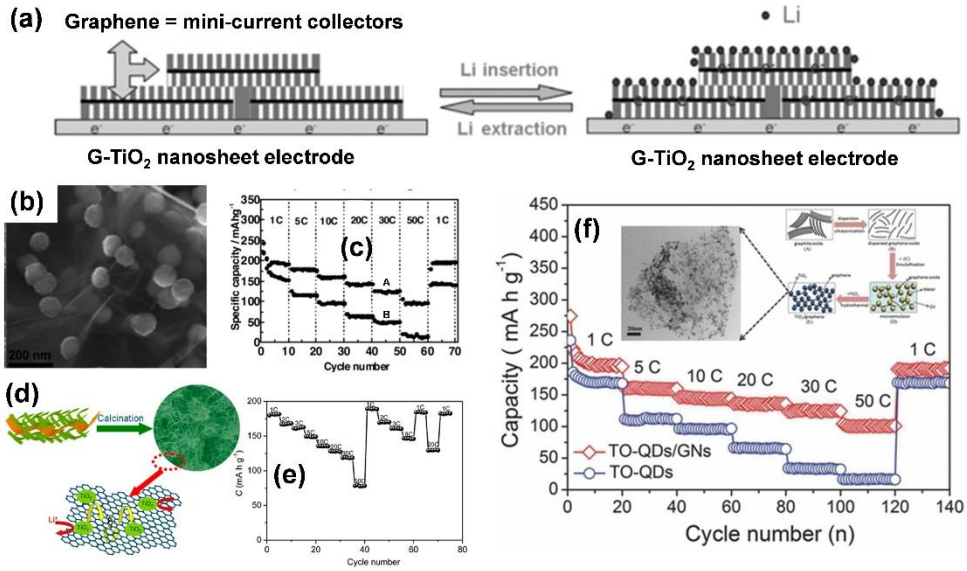

Figure 11. Graphene-based TiO_2 hybrid composites for ultrafast LIBs: (a) Lithium insertion and extraction in G-TiO_2 nanosheets, where graphene acts as mini-current collectors to enhance the electrical conductivity.[29] (b) SEM image of mesoporous anatase TiO_2 nanospheres on graphene sheets; and (c) Comparison of the specific capacity at different rates between (A) TO/GS and (B) TO electrode.[30] (d) Illustration of the processes and growth mechanism of TiO_2-based nanocomposites; and (e) Typical cycling behavior of f-TiO_2/G coin-type cells at various rates.[31] (f) Comparison of the specific capacity at different rates between TiO_2-QDs/GNs and TiO_2-QDs electrodes.[32]

2.2.4 Mechanical support

TiO_2 is an excellent candidate as the anode material for LIBs with low volume variation (<4%) due to its crystal structure. Therefore, it is reasonable to take use of TiO_2 as the backbone or rigid substrate for the large theoretical capacity (e.g., Fe_2O_3, SnO_2, and Si) to alleviate their volume expansion during lithiation/delithiation.[37] For example, hierarchical hollow TiO_2@Fe_2O_3 core-shell nanostructures[38] were fabricated through atomic layer deposition (ALD) and sacrificial template-assisted hydrolysis method, which possessed a large surface area with a hollow interior and robust structure (Figure 12a). TiO_2 herein served as the mechanical support for the whole composite in addition to its contribution to the capacity. This TiO_2@Fe_2O_3 composite anode manifested a high reversible capacity with initial value of 840 mAh g^{-1} and enhanced cycling stability that the capacity of 530 mAh g^{-1} was retained after 200 cycles at the current density of 200 mA g^{-1} (Figure 12b). Similar concept is realized by Feng *et al.*[39] on graphene-based TiO_2/SnO_2 hybrid system, in which TiO_2 was proposed as the component to buffer the excessive volume expansion of SnO_2 during the conversion reaction. Moreover, graphene sheets were integrated into the TiO_2/SnO_2 hybrid to enhance the overall conductivity, overcoming the capacity fading during the cycling of TiO_2/SnO_2 heterostructures (Figure 12c). Thus, the graphene-based TiO_2/SnO_2 hybrid nanosheets exhibited superior reversible capacity and excellent rate capability.

Similar to conversion reaction electrode materials as mentioned, lithium alloy reaction compounds Li_xM (M = Si, Sn, Ge, etc.) are also suffering from huge volume variation upon lithium insertion/extraction process. Taking Si as example, it possesses the highest theoretical capacity of 4200 mAh g^{-1} with the volume expansion by 400%, resulting in degradation of the material structure as well as the loss of contact between the active materials with the current collector. The mechanical degradation will further lead to the capacity loss during cycling, especially at high charge/discharge rates. By using rigid TiO_2-

$_x$/C composite as the scaffold to encapsulate Si nanoparticles inside, Dou *et al.*[40] reported a core-shell structured Si nanoparticles@TiO_{2-x}/C mesoporous microfiber composite (SiNPs@T/C) (Figure 12d), which showed remarkable rate capability that a high capacity of 939 mAh g^{-1} can be delivered even at the current density of 12 A g^{-1}, which is 89% of the initial capacity at 0.2 C (Figure 12e).

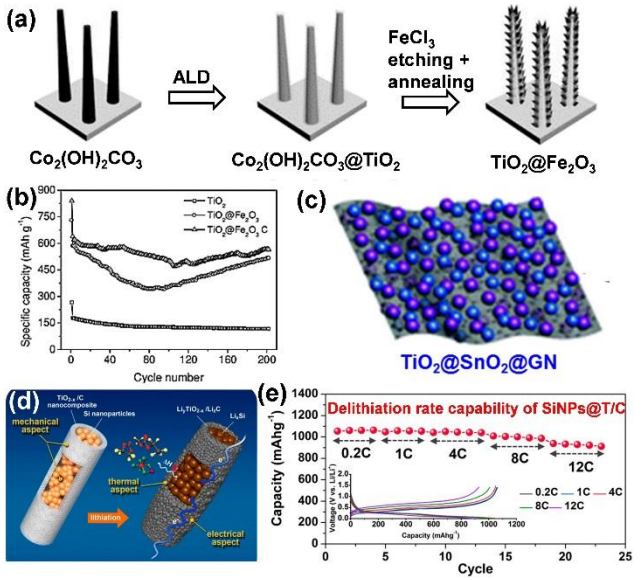

Figure 12. TiO_2 materials combined with other compounds for improved lithium ion storage: (a) Schematic illustration of the preparation process of a hierarchical hollow TiO_2@Fe_2O_3 core-shell nanostructures; and (b) Cycling performance of the electrodes at a current density of 200 mA g^{-1}.[38] (c) Configuration of graphene-based TiO_2/SnO_2 hybrid nanosheets.[39] (d) Schematic illustration of a core-shell structured Si nanoparticles@TiO_{2-x}/C mesoporous microfiber composite as an anode material for LIBs; and (e) Delithiation rate capability of SiNPs@T/C and the corresponding voltage profiles (inset).[40]

3. Conclusion and outlook

In this review, we review the state-of-the-art development of TiO_2 materials towards high performance LIBs. The general concept for achieving high performance LIBs in terms of high safety, long lifetime, high energy density, and high power density are introduced. Following the basic concept, the corresponding materials engineering on TiO_2-based materials to improve their electrochemical performance by intrinsically and extrinsically strategies are presented. From the materials engineering aspect, their forms of existence have an influence on their physicochemical properties, and new concepts and promising approaches are conducted to achieve high performance of TiO_2. For the intrinsic approaches, including exploitation of nanomaterials with high surface areas, structure/morphology optimization, and facet controlling, doping technology, can enhance electron and lithium ion diffusion rates inside or on the surface of the active materials significantly. For the extrinsic approaches, including carbon coating, conductive substrate design, and hybridization with conductive agent, are also play an important role in improving the battery performance in term of rate performance, cycling capability, and capacity.

Although the promising processes have been developed in the past few years, continuous efforts are desired to exploit advanced TiO_2 materials/structure for commercialization. In this case, critical aspects need to be considered to shape the future of TiO_2 as the anode materials. Firstly, due to the intercalation mechanism, the capacity of the TiO_2 materials is still limited (< 350 mAh/g) for the practical application with high energy density demanded. Thus, the development of the high capacity (> 1000 mAh/g) and high rate (> 10 C) TiO_2-based electrode is desirable, and the exploration on the new phase of TiO_2 family or the hybrid structure is needed. Secondly, most of the current research focused on the rational materials engineering for improving the electrode performance, the fundamental study on the thermodynamic and kinetics study of the lithium ion and electron transport inside TiO_2 nanostructures on the lithiation and de-lithiation process is less studied and understood. The study on this direction will provide us the basic guidance on the material design for the TiO_2. Thirdly, towards the commercialization aspect, there is a gap between the lab experiments and the requirements for the practical electrodes, and the reported results on the electrode performance is difficult for the comparison. To fill up this gap, the standard preparation (area mass loading, electrode formulation, etc.) on the electrode towards the practical battery testing is needed to be laid down. Lastly, the safe electrolyte systems with high ionic conductivity and non-flammable property are also important for the high power LIBs. Based on the fundamental understanding on material design principle towards high performance LIBs, continuing efforts and breakthrough concepts are required to overcome the current challenges of TiO_2 anode electrode with high- power and energy density, realizing the commercialization for automotive in the near future.

Yanyan Zhang obtained his B.S. and M.S. degrees at Nanjing University of Aeronautics and Astronautics in 2006 and 2009 respectively. She completed his Ph.D. in 2012 from Nanyang Technological University, Singapore. Currently, she is a research fellow with Prof. Xiaodong Chen at the same university. Her research interest is the development of advanced nanomaterials for photocatalytic water splitting and lithium-ion batteries.

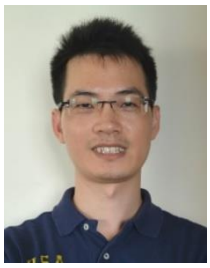

Yuxin Tang obtained his B.S. and M.S. degrees at Nanjing University of Aeronautics and Astronautics in 2006 and 2008 respectively, and completed his Ph.D. in 2012 from Nanyang Technological University, Singapore. Currently, he is a research fellow with Prof. Xiaodong Chen at the same university. His research interest is rational design of advanced functional materials for energy conversion and storage, including lithium-ion batteries, photocatalytic water splitting and water purification, etc.

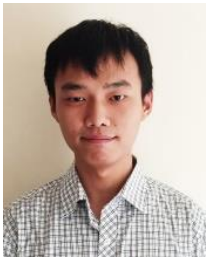

Wenlong Li is currently an undergraduate student in material engineering from Nanyang Technological University, Singapore. He is selected by the URECA (undergraduate research experience on campus) program under Prof. Xiaodong Chen due to academic excellence. His research interest is nanostructured materials for lithium ion batteries.

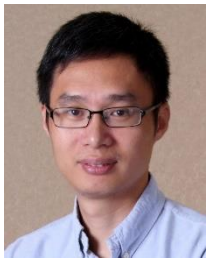

Xiaodong Chen is an Associate Professor at Nanyang Technological University, Singapore. He received his BS degree (Honors) in chemistry from Fuzhou University (China) in 1999, MS degree (Honors) in physical chemistry from the Chinese Academy of Sciences in 2002, and PhD degree (Summa Cum Laude) in biochemistry from University of Muenster (Germany) in 2006. After working as a postdoctoral fellow at Northwestern University (USA), he started his independent research career as a Singapore National Research Foundation Fellow and Nanyang Assistant Professor at Nanyang Technological University in 2009. He was promoted to Associate Professor with tenure in September of 2013. His research interests include programmable materials for energy conversion and integrated nano-bio interface. He is currently an associate editor for Nanoscale.

Acknowledgements

This work was supported by Singapore MOE Tier 2 (MOE2015-T2-1-110) and Singapore National Research Foundation (Nanomaterials for Energy and Water Management CREATE Programme and NRF–POC Grant).

Keywords: TiO_2 nanostructures • lithium ion batteries • high-rate • anode materials • material design

[1] a) B. Dunn, H. Kamath, J. M. Tarascon, *Science* **2011**, *334*, 928-935; b) H. G. Zhang, X. D. Yu, P. V. Braun, *Nat. Nanotech.* **2011**, *6*, 277-281; c) D. Larcher, J. M. Tarascon, *Nat. Chem.* **2015**, *7*, 19-29; d) Y. Tang, Y. Zhang, W. Li, B. Ma, X. Chen, *Chem. Soc. Rev.* **2015**, *44*, 5926-5940; e) Y. Tang, Y. Zhang, X. Rui, D. Qi, Y. Luo, W. R. Leow, S. Chen, J. Guo, J. Wei, W. Li, J. Deng, Y. Lai, B. Ma, X. Chen, *Adv. Mater.* **2016**, *28*, 1567-1576; f) X. Rui, Y. Tang, O. I. Malyi, A. Gusak, Y. Zhang, Z. Niu, H. T. Tan, C. Persson, X. Chen, Z. Chen and Q. Yan, *Nano Energy*, **2016**, *22*, 583-593.

[2] a) K. Kang, Y. S. Meng, J. Bréger, C. P. Grey, G. Ceder, *Science* **2006**, *311*, 977-980; b) M. H. Park, K. Kim, J. Kim, J. Cho, *Adv. Mater.* **2010**, *22*, 415-418; c) S. W. Oh, S. T. Myung, S. M. Oh, K. H. Oh, K. Amine, B. Scrosati, Y. K. Sun, *Adv. Mater.* **2010**, *22*, 4842-4845; d) A. Van der Ven, J. Bhattacharya, A. A. Belak, *Acc. Chem. Res.* **2012**, *46*, 1216-1225; e) F. Lin, I. M. Markus, D. Nordlund, T.-C. Weng, M. D. Asta, H. L. Xin, M. M. Doeff, *Nat. Commun.* **2014**, *5*, 3529; f) M. He, K. Kravchyk, M. Walter, M. V. Kovalenko, *Nano Lett.* **2014**, *14*, 1255-1262; g) W. Weng, Q. Sun, Y. Zhang, S. He, Q. Wu, J. Deng, X. Fang, G. Guan, J. Ren, H. Peng, *Adv. Mater.* **2015**, *27*, 1363-1369; h) C. Wu, X. Lu, L. Peng, K. Xu, X. Peng, J. Huang, G. Yu, Y. Xie, *Nat. Commun.* **2013**, *4*, 2431; i) Y. Zhao, B. Liu, L. Pan, G. Yu, *Energy Environ. Sci.* **2013**, *6*, 2856-2870; j) J. B. Goodenough, K. S. Park, *J. Am. Chem. Soc.* **2013**, *135*, 1167-1176.

[3] a) Z. Chen, I. Belharouak, Y. K. Sun, K. Amine, *Adv. Funct. Mater.* **2013**, *23*, 959-969; b) H. Ren, R. B. Yu, J. Y. Wang, Q. Jin, M. Yang, D. Mao, D. Kisailus, H. J. Zhao, D. Wang, *Nano Lett.* **2014**, *14*, 6679-6684; c) Y. Zhang, Z. Jiang, J. Huang, L. Y. Lim, W. Li, J. Deng, D. Gong, Y. Tang, Y. Lai, Z. Chen, *RSC Adv.* **2015**, *5*, 79479-79510; d) Y. Y. Zhang, Y. X. Tang, S. Y. Yin, Z. Y. Zeng, H. Zhang, C. M. Li, Z. L. Dong, Z. Chen, X. D. Chen, *Nanoscale* **2011**, *3*, 4074-4077.

[4] a) A. Vlad, N. Singh, C. Galande, P. M. Ajayan, *Adv. Energy Mater.* **2015**, *5*, 1402115; b) Y. Tang, X. Rui, Y. Zhang, T. M. Lim, Z. Dong, H. H. Hng, X. Chen, Q. Yan, Z. Chen, *J. Mater. Chem. A* **2013**, *1*, 82-88; c) H. Wang, P. Hu, J. Yang, G. Gong, L. Guo, X. Chen, *Adv. Mater.* **2015**, *27*, 2348-2354; d) H. Yang, Z. Liu, B. K. Chandran, J. Deng, J. Yu, D. Qi, W. Li, Y. Tang, C. Zhang, X. Chen, *Adv. Mater.* **2015**, *27*, 5593-5598; e) Y. Zhang, X. Rui, Y. Tang, Y. Liu, J. Wei, S. Chen, W. R. Leow, W. Li, Y. Liu, J. Deng, B. Ma, Q. Yan, X. Chen, **2016**, *6*, 1502409.

[5] a) B. Wang, Y. Bai, Z. Xing, D. Hulicova-Jurcakova, L. Wang, *ChemNanoMat* **2015**, *1*, 96-101; b) J. Y. Liao, A. Manthiram, *Adv. Energy Mater.* **2014**, *4*, 1400403.

[6] Y. Q. Wang, L. Guo, Y. G. Guo, H. Li, X. Q. He, S. Tsukimoto, Y. Ikuhara, L. J. Wan, *J. Am. Chem. Soc.* **2012**, *134*, 7874-7879.

[7] A. G. Dylla, G. Henkelman, K. J. Stevenson, *Acc. Chem. Res.* **2013**, *46*, 1104-1112.

[8] A. G. Dylla, P. Xiao, G. Henkelman, K. J. Stevenson, *J. Phys. Chem. Lett.* **2012**, *3*, 2015-2019.

[9] M. Park, X. Zhang, M. Chung, G. B. Less, A. M. Sastry, *J. Power Sour.* **2010**, *195*, 7904-7929.

[10] M. L. Sushko, K. M. Rosso, J. Liu, *J. Phys. Chem. C* **2010**, *114*, 20277-20283.

[11] a) Z. X. Yang, G. D. Du, Q. Meng, Z. P. Guo, X. B. Yu, Z. X. Chen, T. L. Guo, R. Zeng, *J. Mater. Chem.* **2012**, *22*, 5848-5854; b) I. Abayev, A. Zaban, F. Fabregat-Santiago, J. Bisquert, *Phys. Status Solidi A-Appl. Res.* **2003**, *196*, R4-R6.

[12] M. Fehse, E. Ventosa, *ChemPlusChem* **2015**, *80*, 785-795.

[13] M. Wagemaker, R. van de Krol, A. P. M. Kentgens, A. A. van Well, F. M. Mulder, *J. Am. Chem. Soc.* **2001**, *123*, 11454-11461.

[14] X. Yan, Y. Li, M. Li, Y. Jin, F. Du, G. Chen, Y. Wei, *J. Mater. Chem. A* **2015**, *3*, 4180-4187.

[15] a) Q. Zhang, E. Uchaker, S. L. Candelaria, G. Cao, *Chem. Soc. Rev.* **2013**, *42*, 3127-3171; b) V. Malgras, Q. Ji, Y. Kamachi, T. Mori, F.-K. Shieh, K. C. W. Wu, K. Ariga, Y. Yamauchi, *Bull. Chem. Soc. Jpn.* **2015**, *88*, 1171-1200; c) Y. Tang, P. Wee, Y. Lai, X. Wang, D. Gong, P. D. Kanhere, T.-T. Lim, Z. Dong, Z. Chen, *J. Phys. Chem. C* **2012**, *116*, 2772-2780; d) X. Rui, Y. Tang, O. I. Malyi, A. Gusak, Y. Zhang, Z. Niu, H. T. Tan, C. Persson, X. Chen, Z. Chen, Q. Yan, *Nano Energy*, doi:10.1016/j.nanoen.2016.1003.1001.

[16] Y. Ren, Z. Liu, F. Pourpoint, A. R. Armstrong, C. P. Grey, P. G. Bruce, *Angew. Chem. Int. Ed.* **2012**, *51*, 2164-2167.

[17] Y. X. Tang, Y. Y. Zhang, J. Y. Deng, J. Q. Wei, H. L. Tam, B. K. Chandran, Z. L. Dong, Z. Chen, X. D. Chen, *Adv. Mater.* **2014**, *26*, 6111-6118.

[18] Y. X. Tang, Y. Y. Zhang, J. Y. Deng, D. P. Qi, W. R. Leow, J. Q. Wei, S. Y. Yin, Z. L. Dong, R. Yazami, Z. Chen, X. D. Chen, *Angew. Chem. Int. Ed.* **2014**, *53*, 13488-13492.

[19] a) G. Q. Zhang, H. B. Wu, T. Song, U. Paik, X. W. Lou, *Angew. Chem. Int. Ed.* **2014**, *53*, 12590-12593; b) Z. Jiang, Y. Tang, Q. Tay, Y. Zhang, O. I. Malyi, D. Wang, J. Deng, Y. Lai, H. Zhou, X. Chen, Z. Dong and Z. Chen, *Adv. Energy Mater.*, 2013, **3**, 1368-1380; c) Y. Zhang, B. Wu, Y. Tang, D. Qi, N. Wang, X. Wang, X. Ma, T. C. Sum, X. Chen, *Small* **2016**, doi:10.1002/smll.201503611; d) H. Ren, J. Sun, R. Yu, M. Yang, L. Gu, P. Liu, H. Zhao, D. Kisailus, D. Wang, *Chem. Sci.* **2016**, *7*, 793-798; e) X. Lai, J. E. Halpert, D. Wang, *Energy Environ. Sci.* **2012**, *5*, 5604-5618; f) N. Yang, Y. Liu, H. Wen, Z. Tang, H. Zhao, Y. Li, D. Wang, *ACS Nano* **2013**, *7*, 1504-1512; g) Q. Jin, Z. Li, K. Lin, S. Wang, R. Xu, D. Wang, *RSC Adv.* **2014**, *4*, 44692-44699; h) J. Qi, X. Lai, J. Wang, H. Tang, H. Ren, Y. Yang, Q. Jin, L. Zhang, R. Yu, G. Ma, Z. Su, H. Zhao, D. Wang, *Chem. Soc. Rev.* **2015**, *44*, 6749-6773.

[20] a) J. Maier, *Angew. Chem. Int. Ed.* **2013**, *52*, 4998-5026; b) J. Jamnik, J. Maier, *Phys. Chem. Chem. Phys.* **2003**, *5*, 5215-5220.

[21] Q. L. Wu, J. G. Xu, X. F. Yang, F. Q. Lu, S. M. He, J. L. Yang, H. J. Fan, M. M. Wu, *Adv. Energy Mater.* **2015**, *5*, 9.

[22] a) H. G. Yang, C. H. Sun, S. Z. Qiao, J. Zou, G. Liu, S. C. Smith, H. M. Cheng, G. Q. Lu, *Nature* **2008**, *453*, 638-641; b) J. S. Chen, Y. L. Tan, C. M. Li, Y. L. Cheah, D. Y. Luan, S. Madhavi, F. Y. C. Boey, L. A. Archer, X. W. Lou, *J. Am. Chem. Soc.***2010**, *132*, 6124-6130.

[23] C. H. Sun, X. H. Yang, J. S. Chen, Z. Li, X. W. Lou, C. Li, S. C. Smith, G. Q. Lu, H. G. Yang, *Chem. Commun.* **2010**, *46*, 6129-6131.

[24] S. T. Myung, M. Kikuchi, C. S. Yoon, H. Yashiro, S. J. Kim, Y. K. Sun, B. Scrosati, *Energy Environ. Sci.* **2013**, *6*, 2609-2614.

[25] T. Xia, W. Zhang, J. B. Murowchick, G. Liu, X. B. Chen, *Adv. Energy Mater.* **2013**, *3*, 1516-1523.

[26] a) J. S. Cho, Y. J. Hong, Y. C. Kang, *Chemistry – A European Journal* **2015**, *21*, 11082-11087; b) J. Y. Liao, D. Higgins, G. Lui, V. Chabot, X. C. Xiao, Z. W. Chen, *Nano Lett.* **2013**, *13*, 5467-5473.

[27] a) M.-S. Balogun, W. Qiu, Y. Luo, Y. Huang, H. Yang, M. Li, M. Yu, C. Liang, P. Fang, P. Liu, Y. Tong, *ChemElectroChem* **2015**, *2*, 1243-1248; b) K. S. Park, J. G. Kang, Y. J. Choi, S. Lee, D. W. Kim, J. G. Park, *Energy Environ. Sci.* **2011**, *4*, 1796-1801; c) F. Bonaccorso, L. Colombo, G. Yu, M. Stoller, V. Tozzini, A. C. Ferrari, R. S. Ruoff, V. Pellegrini, *Science* **2015**, 347, 1246501; d) Y. Shi, L. Peng, Y. Ding, Y. Zhao, G. Yu, *Chem. Soc. Rev.* **2015**, *44*, 6684-6696; e) P. Xiong, B. Liu, V. Teran, Y. Zhao, L. Peng, X. Wang, G. Yu, *ACS Nano* **2014**, *8*, 8610-8616.

[28] W. Wang, M. Tian, A. Abdulagatov, S. M. George, Y. C. Lee, R. G. Yang, *Nano Lett.* **2012**, *12*, 655-660.

[29] S. B. Yang, X. L. Feng, K. Mullen, *Adv. Mater.* **2011**, *23*, 3575-3579.

[30] N. Li, G. Liu, C. Zhen, F. Li, L. L. Zhang, H. M. Cheng, *Adv. Funct. Mater.* **2011**, *21*, 1717-1722.

[31] X. Xin, X. F. Zhou, J. H. Wu, X. Y. Yao, Z. P. Liu, *Acs Nano* **2012**, *6*, 11035-11043.

[32] R. W. Mo, Z. Y. Lei, K. N. Sun, D. Rooney, *Adv. Mater.* **2014**, *26*, 2084-2088.

[33] V. Etacheri, J. E. Yourey, B. M. Bartlett, *ACS Nano* **2014**, *8*, 1491-1499.

[34] W. Li, F. Wang, Y. P. Liu, J. X. Wang, J. P. Yang, L. J. Zhang, A. A. Elzatahry, D. Al-Dahyan, Y. Y. Xia, D. Y. Zhao, *Nano Lett.* **2015**, *15*, 2186-2193.

[35] B. C. Qiu, M. Y. Xing, J. L. Zhang, *J. Am. Chem. Soc.***2014**, *136*, 5852-5855.

[36] M. N. Hyder, B. M. Gallant, N. J. Shah, Y. Shao-Horn, P. T. Hammond, *Nano Lett.* **2013**, *13*, 4610-4619.

[37] Z. W. Seh, W. Y. Li, J. J. Cha, G. Y. Zheng, Y. Yang, M. T. McDowell, P. C. Hsu, Y. Cui, *Nat. Commun.* **2013**, *4*, 1331.

[38] J. S. Luo, X. H. Xia, Y. S. Luo, C. Guan, J. L. Liu, X. Y. Qi, C. F. Ng, T. Yu, H. Zhang, H. J. Fan, *Adv. Energy Mater.* **2013**, *3*, 737-743.

[39] Y. P. Tang, D. Q. Wu, S. Chen, F. Zhang, J. P. Jia, X. L. Feng, *Energy Environ. Sci.* **2013**, *6*, 2447-2451.

[40] G. Jeong, J. G. Kim, M. S. Park, M. Seo, S. M. Hwang, Y. U. Kim, Y. J. Kim, J. H. Kim, S. X. Dou, *ACS Nano* **2014**, *8*, 2977-2985.

Table of Contents

FOCUS REVIEW

In this review, we present the state-of-the-art materials design strategies for TiO_2 materials to achieve high performance lithium-ion batteries. Continuing efforts and breakthrough concepts are still required to achieve TiO_2 anode electrode with high- power and energy density, realizing the commercialization for automotive in the near future.

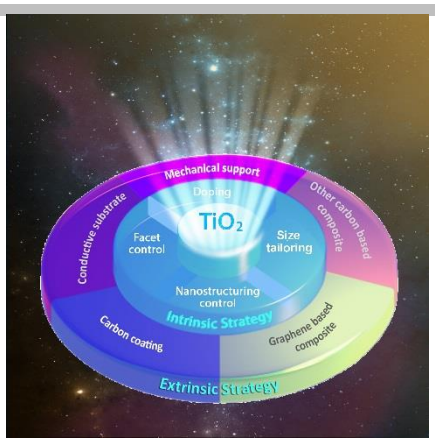

*Yanyan Zhang, Yuxin Tang, Wenlong Li, and Xiaodong Chen**

Page No. – Page No.

Nanostructured TiO_2-based Anode Materials for High-performance Rechargeable Lithium-ion Batteries